AN INVESTIGATION OF WIRE GRID AND SURFACE PATCH MODELING USING THE NUMERICAL ELECTROMAGNETICS CODE (NEC)

James K. Breakall
Electrical and Computer Engineering Department
The Pennsylvania State University
University Park, PA 16802

Richard W. Adler and Panos D. Elliniadis
Electrical and Computer Engineering Department
Naval Postgraduate School
Monterey, CA 93943

ABSTRACT

The Numerical Electromagnetics Code (NEC) was used to evaluate the admittance and the electric near and far fields of a monopole antenna mounted on a cubical box over a perfectly conducting ground plane. Two models of the box, employing surface patches and wire grids, were evaluated. The monopole was positioned at the center, the edge, and at a corner of the box's top surface. NEC admittance results were obtained and good agreement was found with experimental data and with results from PATCH, another independent electromagnetic modeling code. Results are presented in contour and 3-D formats for the near fields and polar format for the far field radiation patterns using surface patch and wire grid models in NEC. Excellent agreement was obtained for both approaches in NEC after finding the optimum number of patches and wire grid segmentation to obtain convergence. This paper provides guidelines for convergence for both modeling approaches and indicates a six-fold savings in run-time for the surface patch method. Furthermore, results are presented in modern graphical format for near field comparisons of the two NEC techniques.

I. INTRODUCTION

The Method of Moments technique is the theoretical basis for the Numerical Electromagnetics Code (NEC), which is a code for the simulation and analysis of the electromagnetic response of antennas and other metallic structures [1]. NEC is the computer simulation tool that was used in this investigation of near fields.

Experimental and computational investigations were previously performed to determine the admittance characteristics of a monopole antenna mounted on a cubical conducting box of 0.1 m sides ($\lambda/3$ at a frequency of 1 GHz) over a ground plane [2,3]. This simple geometrical model was used to simulate the basic shipboard topside environment of a ship's superstructure. The antenna, a 6 cm monopole ($\lambda/5$ at the same frequency of 1

GHz), was tested for three different mounting positions on the top surface. Experimental data and numerically calculated results using the PATCH computer code of admittance for the 6 cm monopole antenna were presented versus frequency. PATCH is a recently developed frequency domain electromagnetic analysis code based on a Method of Moments solution to the Electric Field Integral Equation (EFIE) [4]. In this code objects are modeled by planar triangular patches which easily conform to surfaces and boundaries of general shape and allow variable patch densities over the surface of the object. This code can model open as well as closed surfaces which is a major advantage over previous Magnetic Field Integral Equation (MFIE) patch codes which only could model closed surfaces.

In this paper, the Numerical Electromagnetics Code (NEC) is used to evaluate the admittance and also the electric near and far field structure of the 6 cm monopole antenna mounted on the cubical box.

Convergence results are obtained and presented offering possible guidelines for more complex models. Also, this paper will present results of near fields for both surface patches and wire grid models in NEC using modern graphical formats. Additionally, it has been found in this paper that wire grid models take as much as six times the run-time of like surface patch models in NEC. It is hoped that all of these findings can form the basis of useful guidelines for further modeling of complex objects using NEC.

II. BACKGROUND

The fields around an antenna may be divided into two regions, one near the antenna called the near field or Fresnel zone and one at a large distance called the far field or Fraunhofer zone [5]. The usually specified boundary between the near field and far field is the distance, $r=2D^2/\lambda$ where D is the maximum length of the antenna in meters and λ is the wavelength in meters. The distance from the surface of the antenna to this boundary is called the near field region, while beyond this boundary the region is called the far field. The near field region can be further divided into two subregions, the reactive and radiating near field. The reactive near field usually extends to $\lambda/2\pi$ from the antenna's surface, while in practice a distance of λ is used to represent this boundary. The phase of the magnetic and electric field is almost in quadrature in regions within a wavelength of the antenna (reactive near field). Beyond the distance of a wavelength, the electric and magnetic fields are propagating in phase (radiating near field) until the far field is reached. In the far field, the shape of the field pattern is independent of the distance, while in the near field the shape depends on this distance.

A description of the numerical codes used in this and the previous work follows. PATCH and NEC are both method of moments computer codes based on either/or both the EFIE or MFIE solutions of the full boundary solution of Maxwell's equations for current density on either cylindrical conductors (wires) or infinitesimally thin flat plates (patches).

PATCH, used in the work reported previously, will calculate both electromagnetic scattering and radiation from objects of arbitrary shape using the EFIE method. This allows modeling objects that are either open or closed and uses planar triangular patches conforming to the surface of the body. The numerical implementation in the code uses subdomain basis expansion functions placed on adjacent pairs of the triangular patches in the Method of Moments procedure. Details concerning this formulation can be found in [6].

NEC, will calculate both electromagnetic scattering and radiation for thin-wire structures of small cylindrical volume using the EFIE method or large closed voluminous and smooth bodies using the MFIE method. For thin structures such as plates or objects which have an opening, the EFIE method provides reasonable accuracy with wire grids having adequate spacing density. A coupled hybrid approach of both EFIE and MFIE is used to model structures containing both wires and closed surfaces and allows a connection of the wires to the surface. Details concerning the derivation of these methods can be found in [7]. Other details involving the choice of the basis functions, current and charge conditions, and capabilities used in NEC can be found in [8,9,10,11,12].

NEC and PATCH both will give solutions for current distributions as mentioned and therefore impedance and admittance at the feedpoint of a voltage excitation. This paper compares surface patch results from NEC with those from PATCH and measurements on values of admittance versus frequency. Wire grid modeling comparisons for admittance using NEC have been performed previously [13]. Furthermore, this work here computes near and far field results which are produced with both wire grid and surface patch modeling in NEC and it is hoped that they can be used to further validate PATCH and other codes.

III. RESULTS

The optimum model for complex structures can be estimated by varying the segment and patch density and observing the results and the convergence of the solution [14]. In the case of an edge-mounted antenna, the accuracy of the results is expected to depend upon the size of the segments and patches near the edge. Smaller segments and patches are suggested at edge areas since the current magnitude may vary rapidly in this region.

The numerical model of a cubical five-sided box of 0.1 meters per side was constructed using NEC (the bottom was not included as a surface since the box was placed on a perfectly conducting ground plane). A 6 cm monopole antenna was placed at the center, at the edge (3.63 cm from center) and at a corner (5.14 cm on a diagonal from center), as shown in Figures 1a and 1b for wire grids and patches respectively.

The first part of the investigation checked the input impedance using NEC as patch density was varied. The number of patches on the top of the box was varied in search of an optimum value of surface samples, which would later be used for near field calculations.

The top was subdivided to retain symmetry, as much as possible, and to closely match positions of the antenna on the experimental model.

A. Monopole at the Center

The monopole was divided into five segments and placed at the center of the top surface. The top surface was divided into 25 (5x5), 49 (7x7), 81 (9x9), and 121 (11x11) patches. Varying the subdivision of the top surface in this manner provided convergence in the results which can easily be seen in Figures 2a and 2b for conductance and susceptance, respectively. Since the current density will change most rapidly at the connection of the monopole, the subdivision of the connection patch is automatically divided by four. It was found that convergence was obtained with the 9x9 subdivision and the correlation of NEC and PATCH results with the measurements is quite good as shown in Figure 2c.

B. Monopole at the Edge

The monopole was attached to an edge at a distance 3.63 cm from the center which corresponds closely to the actual configuration. The difference in distance for the position of the monopole in the NEC model compared to the actual physical geometry is 0.13 cm. A subdivision of the top surface into 81 (9x9) patches produced well-converged results. In Figure 3a are shown the NEC results as well as measurements and PATCH results. It can be seen that good agreement is obtained with measurements and PATCH's conductance values. NEC and PATCH have almost identical performance for susceptance as compared to measurements.

C. Monopole at Corner

The 6 cm monopole in the NEC model was placed at the corner, 5.14 cm on the diagonal from the center and fed at the base. The position of the monopole for the experimental model was 5.15 cm. The top surface was divided into 121 (11x11) patches to obtain well-converged results.

NEC and PATCH results compared to measurements are presented in Figure 3b. NEC is in excellent agreement with PATCH and measurements in both conductance and susceptance, and in the range of 1.15 to 1.40 GHz, both codes are virtually identical.

D. Near Electric Field

Near fields are more difficult to calculate in NEC than far fields. When calculating radiation in close proximity to an antenna, terms in the field expressions with powers of $1/r^2$ (r is the distance from the origin of the antenna to the field point) are appreciable in magnitude compared to the 1/r dependent terms which are dominant in the far field. The near field is thus very dependent on the charge density and the current while the far field is mainly dependent on the current.

For near field calculations, NEC computes the magnitude and phase of each component, E_x, E_y, and E_z separately and a modification was made to also calculate the magnitude of the peak electric field (E-Total) in (V/m), which is the vector sum of the three components E_x, E_y, and E_z. Using the optimum models in NEC for the monopole at the center (9x9 patches), at the edge (9x9 patches), and the corner (11x11 patches), the near field was investigated.

In order to compare NEC near fields for the monopole on the box with known theoretical understanding, we consider a linear current element $I=I_0e^{j\omega t}$ of length z oriented in the z direction and with amplitude I_0 located at the origin as in Figure 4. This antenna is a known simple radiating structure but it will demonstrate basic properties of the near electric field for all small linear antennas. The complete electric field intensity of the antenna is:

$$\bar{E} = \frac{-I_0 \Delta z}{2\pi} j \frac{\sqrt{\mu_0}}{k_0\sqrt{\epsilon_0}} \cos\theta \left(\frac{jk_0}{r^2} + \frac{1}{r^3}\right) e^{-jk_0 r} \bar{i}_r + \frac{-I_0 \Delta z}{4\pi} j \frac{\sqrt{\mu_0}}{k_0\sqrt{\epsilon_0}} \sin\theta \left(\frac{-k_0^2}{r} + \frac{jk_0}{r^2} + \frac{1}{r^3}\right) e^{-jk_0 r} \bar{i}_\theta \quad (1)$$

The only part of the field dominant in the expression for the far field radiated power is that part consisting of the terms varying as r^{-1}, that is

$$\bar{E} = \frac{jk_0 I_0 \Delta z \sqrt{\mu_0}}{4\pi r\sqrt{\epsilon_0}} \sin\theta e^{-jk_0 r} \bar{i}_\theta \quad (2)$$

The parts of the field varying as r^{-2} and r^{-3} are important in the near field. Consequently the terms that are functions of distance r of the E-Field in the above equations are:

$$\left(-\frac{k_0^2}{r} + j\frac{k_0}{r^2} + \frac{1}{r^3}\right) \quad \text{along the x or y-axis} \quad (3a)$$

$$\left(\frac{jk_0}{r^2} + \frac{1}{r^3}\right) \quad \text{along the z-axis.} \quad (3b)$$

All the other terms are phase terms or constants. Generally, the magnitude of the electric field has an r-dependence which can be expressed as:

$$|E(r)| = c\sqrt{\left(\frac{1}{r^3} - \frac{k_0^2}{r}\right)^2 + \left(\frac{k_0}{r^2}\right)^2} \qquad \text{along the x or y-axis} \tag{4a}$$

$$|E(r)| = c\sqrt{\left(\frac{1}{r^3}\right)^2 + \left(\frac{k_0}{r^2}\right)^2} \qquad \text{along the z-axis} \tag{4b}$$

where c is a proportionality constant used to normalize the electric field to the starting position.

FORTRAN programs were developed to plot the magnitude and phase contours of the near electric field using NEC output data [14]. For reference, two simple antennas with analytical results are examined: (1) a 0.15 m ($\lambda/2$) dipole antenna in free space, and (2) a 0.06 m ($\lambda/5$) monopole antenna over a perfect ground plane which corresponds to the same monopole mounted on the cubical box. The near electric field contours are displayed in a section of a plane in 3-dimensional space. The results are shown in Figures 5a and 5b. It is seen that the shape of near electric field is the same for the dipole and monopole antennas. The ratio of the maximum current for the dipole to the monopole as computed by NEC with both fed from a 1 Volt excitation source is -7.0 dB. Therefore, absolute field values for the dipole should be increased by 7.0 dB to make comparisons to the monopole fields with both having the same current. The phase plots of the electric fields for the $\lambda/2$ dipole and 0.06 m monopole are shown in Figures 6a and 6b and show that both antennas have a smooth spherical wavefront pattern.

NEC solutions of the near electric field of the monopole on the box center are shown in Figures 7a and 7b for the magnitude of the total electric field and the phase of the E_z component. The formation of maxima and nulls can also be observed. A maximum occurs at 60° in elevation from the box surface while a null is seen at about 30°. The main lobe starts to develop at a distance 1λ (0.3m) from the antenna. Beyond this point, the main lobe has the same shape independent of distance. Within a distance of 2λ the pattern shape has not yet fully developed.

In order to gain insight into the electric near field variations and where the maxima and minima occur, a 3-dimensional plot is presented in Figure 8. The plot displays a surface whose elevation points represents field strength in the upper portion, and a normal 2-D contour plot "projection" in the lower portion. In this figure the vertex that corresponds to the pointed "spike-like" area of the surface is the origin where the antenna is mounted. The decay of the field as the observation point moves away from the monopole source is expected. The null "trough" can easily been seen in this type of representation.

Figures 9a and 9b show results for the edge-mounted monopole in the same format as the center-mounted case. The following comments will amplify differences from the center case and interesting features of the field distributions. The edge-mounted geometry provides a larger planar surface (box top) in front of the monopole view plane and results in the following differences with respect to the center-mounted geometry:

1. The z-axis peak field is somewhat greater at given distances from the box surface. This is caused by a larger E_x component.

2. The elevation plane null is not as deep.

3. The phase contours for the z component show evidence of two close-in nulls, but very small "phase wrinkles" beyond the near zone.

4. The contour plot depicts a more uniform field overall, with a less severe null.

The corner-mounted monopole near field plots are in Figures 9c and 9d. The fields for this case fall in between the center and edge-mounted field configurations. That is:

1. The elevation plane null is between the nulls of the other two configurations.

2. "Phase wrinkles" show one null, as does the center-mounted case, but it is not as severe.

3. Contour plots indicate a wider field pattern with a fairly uniform distribution away from the monopole.

E. Far Field

Far field radiation patterns were calculated and are presented in Figures 10a and 10b (Monopole at center), 10c and 10d, (Monopole at edge), and 10e and 10f, (Monopole at corner). In Figure 10a, the vertical pattern of the monopole at the center shows that the maximum gain is very close to 5.15 dBi, the theoretical value for a monopole over an infinite perfectly conducting ground plane. In Figure 10b, the horizontal pattern shows omnidirectional radiation from the electrically small box-monopole configuration which is not expected to contribute much directionality in azimuth.

The results of vertical and horizontal patterns for the edge-mounted monopole (Figures 10c and 10d) and the corner-mounted monopole (Figures 10e and 10f) display unsymmetrical patterns.

F. Wire Grid Modeling

Solid surfaces can be modeled in NEC with a grid of wires, with the restriction that the grid cells are to be small in terms of a wavelength. Wire grid modeling guidelines are given in [1,15,16]. For the wire grid modeling technique, typical run-times of the box-monopole configuration have been found to take up to six times those of the surface patch models. The box of Figure 1 is modeled as a five-sided wire grid box of 0.1 m ($\lambda/3$ at 1 GHz) per side having cells of 0.0125 by 0.0125 meters. The 0.06 m monopole antenna was divided into 5 segments and placed on top of the wire grid box at the center, edge (3.75 cm from center) and corner (5.3 cm on the diagonal). The antenna was fed at the base segment for all cases. The wire grid geometry of [13] was used for calculations of the near electric field in the present study. This geometry produced good results for admittance compared with experimental data [2,3]. Magnitude and phase contour plots of near electric field for the wire grid box case with the same field point locations used in the surface patch model are shown for the monopole mounted at the center. The excellent agreement of near fields (Figures 11a and 11b) for the wire grid box with the center-mounted monopole to those of the surface patch model (Figures 7a and 7b) attests to the equivalence of the two numerical models. Differences are less than 1 dB, a value which is difficult to measure. The other wire grid cases for the monopole at the edge and corner also were compared to the surface patch models and excellent agreement was likewise obtained with differences of 1 to 1.5 dB [14]. The differences are expected to be attributed to a more accurate rendition of edge effects for the wire grid model versus the patch model.

IV. CONCLUSIONS

The goal of this investigation was to accurately predict admittance, near and far fields using the Numerical Electromagnetics Code (NEC).

Since few validation benchmark results for near fields were available, an exercise was undertaken using NEC in order to determine optimum models. Box-like structures were analyzed using surface patch and wire grid modeling techniques. The simulation models consisted of a $\lambda/5$ monopole mounted on the top of a $\lambda/3$ box at three different locations: center, edge, and corner. Optimum models were selected by varying the patch density on the top surface of the box and observing the convergence of the solution and comparison with measurements and PATCH results for input admittance, in order to ensure the validity of the models and improve the confidence in near field predictions. Optimum NEC models for the three different mounting geometries were found to be:

- CENTER and EDGE: 9x9 = 81 patches on top (0.0013 λ^2 patch area)
- CORNER: 11x11 = 121 patches on top (0.0009 λ^2 patch area)

Even though edges are not modeled in the surface patch technique [1], this study proves that, for positions very close to an edge, good results can be obtained by careful subdividing (no special subdivision of smaller patches in the vicinity of the edge or corner was required).

Algorithms were developed to produce near electric field (magnitude and phase) contours and 3-D plots [14]. The near field for the monopole on the box has similar characteristics in magnitude and phase as the monopole over a ground plane except in the region where nulls occur from box radiation and diffraction effects. The edge/corner-mounted geometries produced slightly different near field contours compared to the center-mounted geometry. Surface patch and wire grid models for NEC gave essentially similar results for near fields.

Previously, generalized guidelines for near field modeling had not been developed for NEC and the use of wire grid and surface patch modeling for near field determination was approached with caution. Guidelines developed in this study, as well as the results of the near field behavior of the monopole antenna on the conducting box, can be used for future investigations on more complex structures.

The present study is an important step in the direction of modeling the effects of the near field of antenna structures.

REFERENCES

[1] G. J. Burke and A. J. Poggio, "Numerical electromagnetics code (NEC) - Method of Moments," Naval Ocean Systems Center, Tech. Document 116, January 1980.

[2] S. Bhattacharya, "A study of the admittance characteristics of a monopole antenna attached to a conducting box," Master's Thesis, University of Houston, pp. 11-13, pp. 71-73 and pp. 86-88, May 1986.

[3] S. Bhattacharya, S. A. Long, and D. R. Wilton, "The input impedance of a monopole antenna mounted on a cubical conducting box," *IEEE Trans. Antennas Propagat.*, vol. AP-35, No. 7, pp. 756-761, July 1987.

[4] W. A. Johnson, D. R. Wilton, and R. M. Sharpe, "Patch code user's manual," Sandia National Laboratories, Rep. SAND87-2991, May 1988.

[5] A. D. Yaghjian, "An overview of near-field antenna measurements," *IEEE Trans. Antennas Propagat.*, vol. AP-34, No. 1, pp. 30-43, January 1986.

[6] S. M. Rao, D. R. Wilton, and A. W. Glisson, "Electromagnetic scattering by surfaces of arbitrary shape," *IEEE Trans. Antennas Propagat.*, vol. AP-30, No. 3, pp. 409-418, May 1982.

[7] A. J. Poggio and E. K. Miller, "Integral equation solutions of three-dimensional scattering problems," Chapt. IV in *Computer Techniques for Electromagnetics*, Edited by R. Mittra, Pergamon Press, NY, 1973.

[8] J. K. Breakall, G. J. Burke, and E. K. Miller, "The Numerical Electromagnetics Code (NEC)," EMC Symposium & Exhibition, Zurich, Switzerland, March 1985.

[9] Y. S. Yeh and K. K. Mei, "Theory of conical equiangular spiral antennas," Part I - Numerical Techniques, *IEEE Trans. Antennas Propagat.*, vol. AP-15, No. 5, p. 634, September 1967.

[10] A. R. Neureuther et al., "A comparison of numerical methods for thin wire antennas," presented at the 1968 Fall URSI Meeting, Dept. of Electrical Engineering and Computer Sciences, University of California, Berkeley, 1968.

[11] E. K. Miller, R. M. Bevensee, A. J. Poggio, R. Adams, and F. J. Deadrick, "An evaluation of computer programs using integral equations for the electromagnetic analysis of thin wire structures," Lawrence Livermore Nat. Lab. Rep. UCRL-75566, March 1974.

[12] N. C. Albertsen, J. E. Hansen, and N. E. Jencen, "Computation of spacecraft antenna radiation patterns," The Technical University of Denmark, June 1972.

[13] C. R. Molina, "Numerical electromagnetic models of cube-shaped boxes - An investigation for near field prediction of HF shipboard environments," Master's Thesis, Naval Postgraduate School, Monterey, California, December 1987.

[14] P. D. Elliniadis, "An investigation of near fields for HF shipboard antennas - Surface patch and wire grid modeling using the Numerical Electromagnetics Code," Master's Thesis, Naval Postgraduate School, Monterey, California, December 1988.

[15] G. J. Burke, "Enhancements and limitations of the code NEC for modeling electrically small antennas," Lawrence Livermore Nat. Lab. Rep. UCID-20970, January 1987.

[16] G. J. Burke, "Treatment of small wire loops in the Method of Moments code NEC," Lawrence Livermore Nat. Lab. Rep. UCID-21196, October 1987.

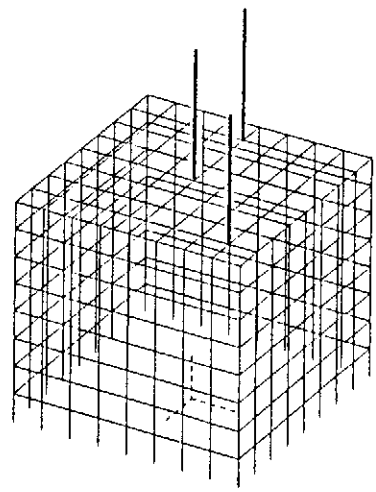

THETA = 60.00 PHI = 30.00 ETA = 90.00

Figure 1a. Monopole at the Center, Edge, and Corner of the Wire Grid Box Model.

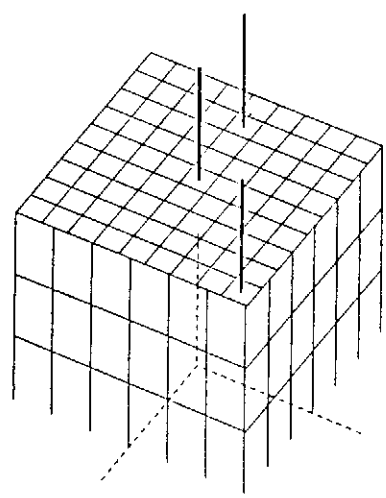

THETA = 45.00 PHI = 30.00 ETA = 90.00

Figure 1b. Monopole at the Center, Edge, and Corner of the Surface Patch Box Model.

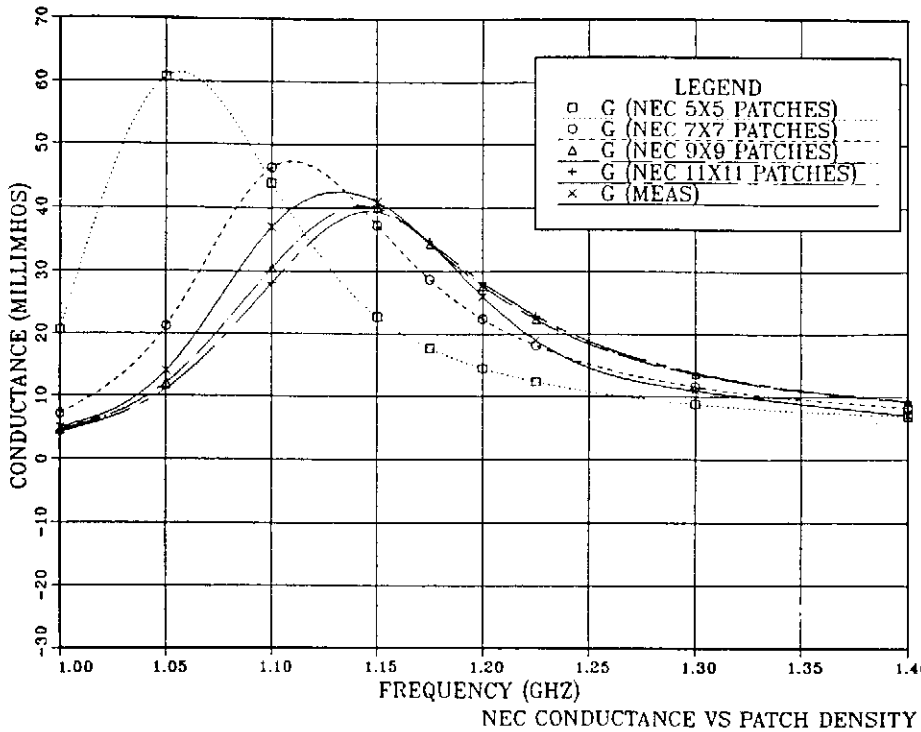

Figure 2a. Monopole at Center of Patch Box, NEC Conductance vs. Patch Density.

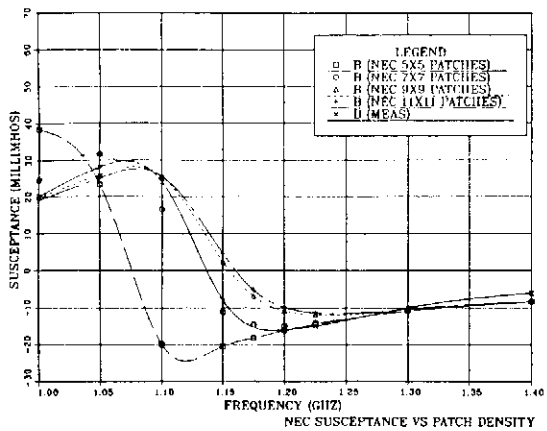

Figure 2b. Monopole at Center of Patch Box, NEC Susceptance vs. Patch Density.

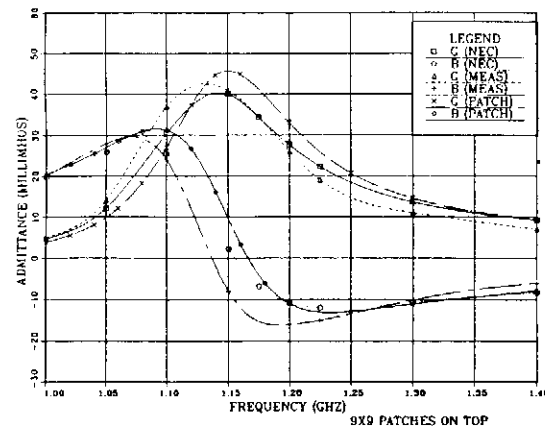

Figure 2c. Monopole at Center of Patch Box, NEC Admittance vs. Measurements and PATCH Code.

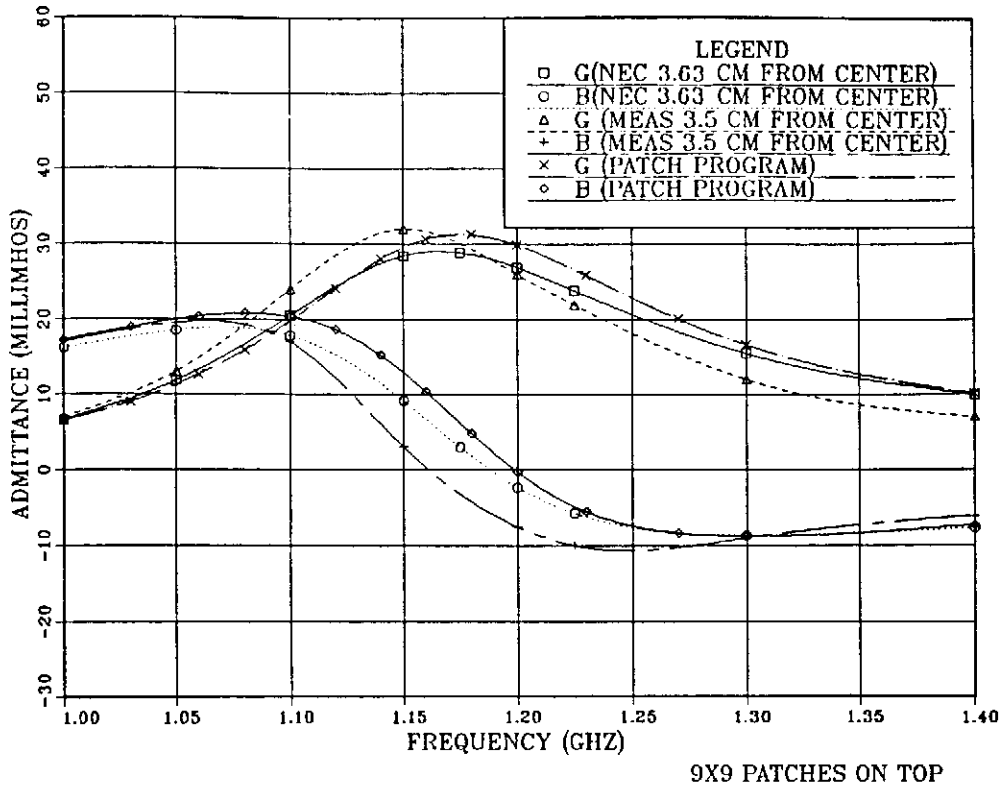

Figure 3a. Monopole at Edge of Patch Box, NEC Admittance vs. Measurements and PATCH Code.

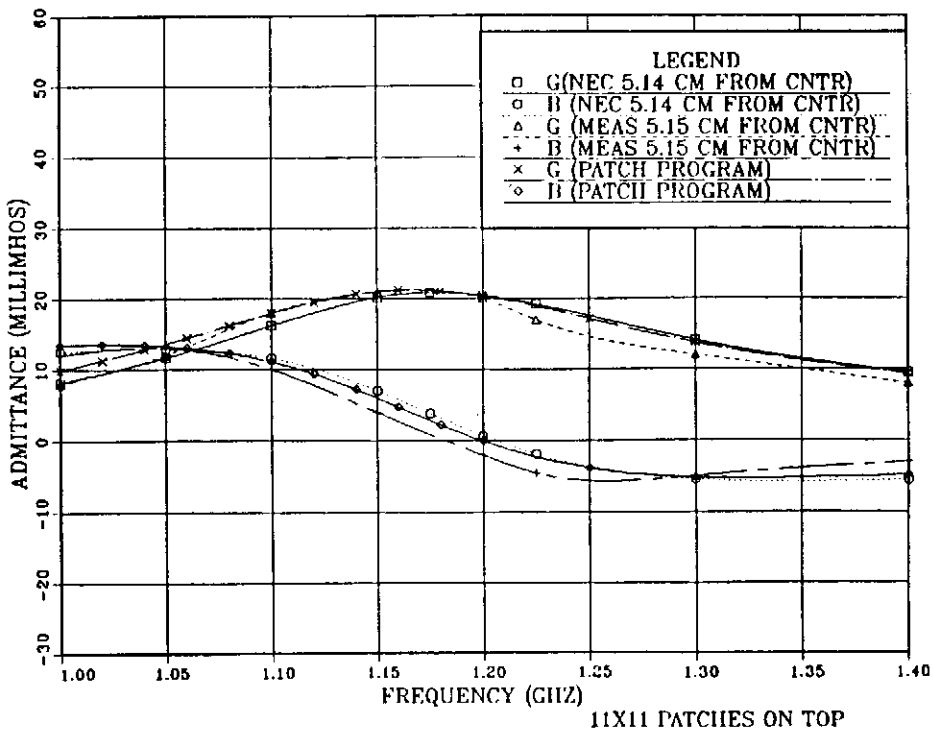

Figure 3b. Monopole at Corner of Patch Box, NEC Admittance vs. Measurements and PATCH Code.

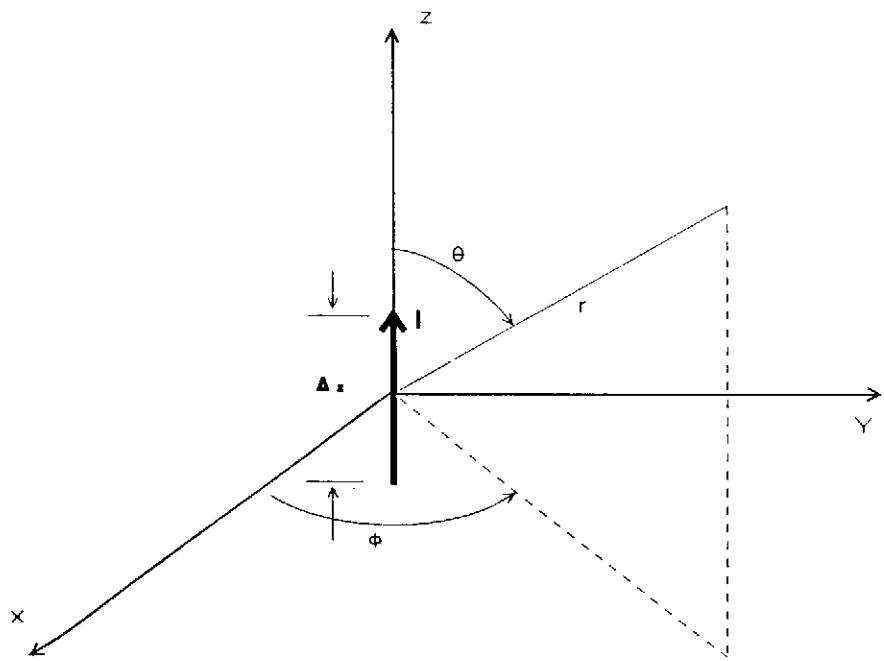

Figure 4. A Linear Current Radiator.

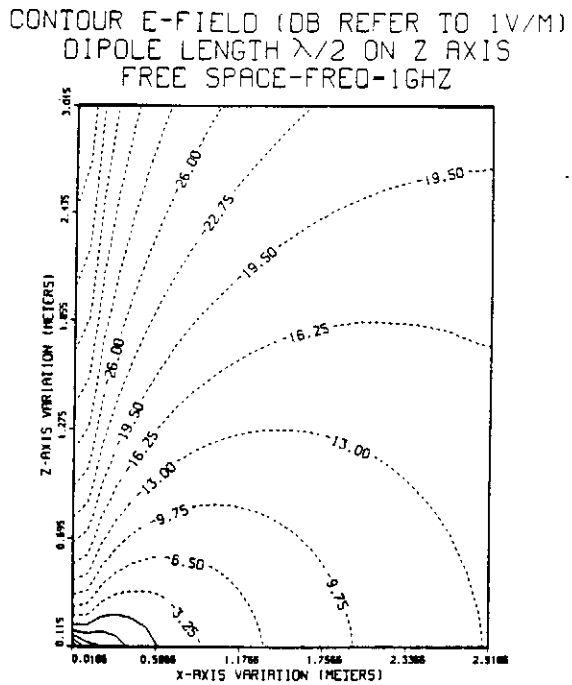

Figure 5a. Total E-Field Contours, Dipole λ/2 on Z-Axis in Free Space.

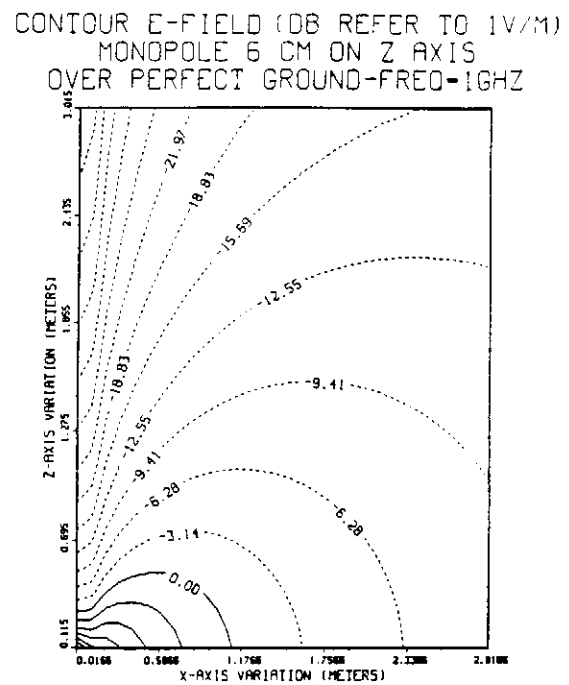

Figure 5b. Total E-Field Contours, Monopole 6 cm Over Perfect Ground.

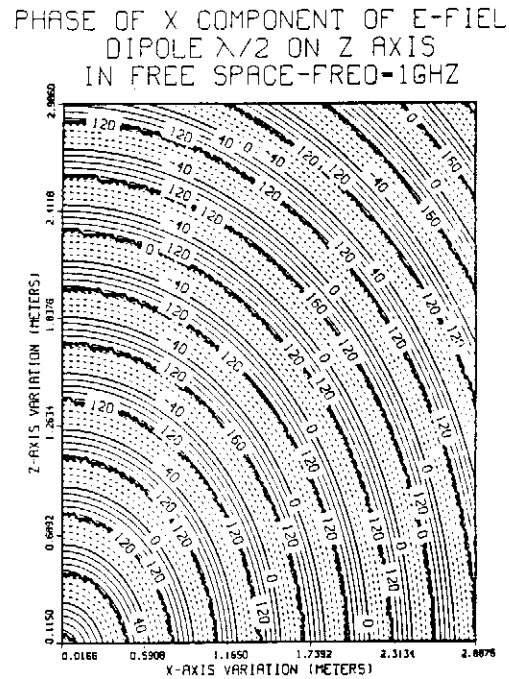

Figure 6a. Z-Component, E-Field Phase Contours, Dipole λ/2 in Free Space.

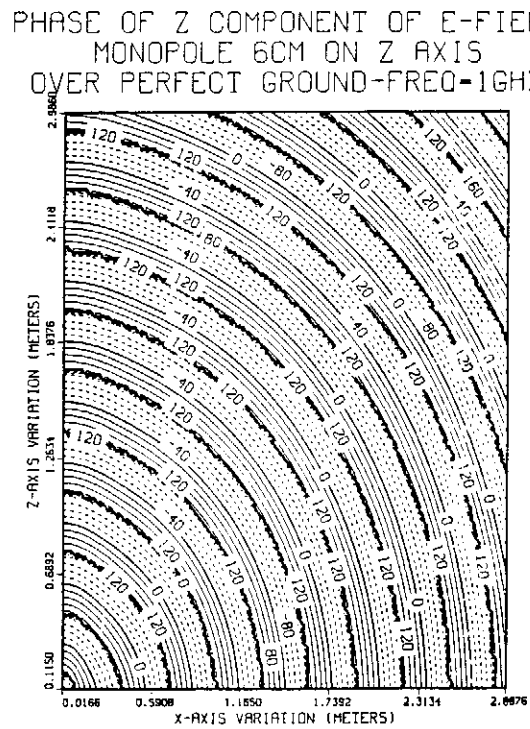

Figure 6b. Z-Component, E-Field Phase Contours, Monopole 6 cm Over Perfect Ground.

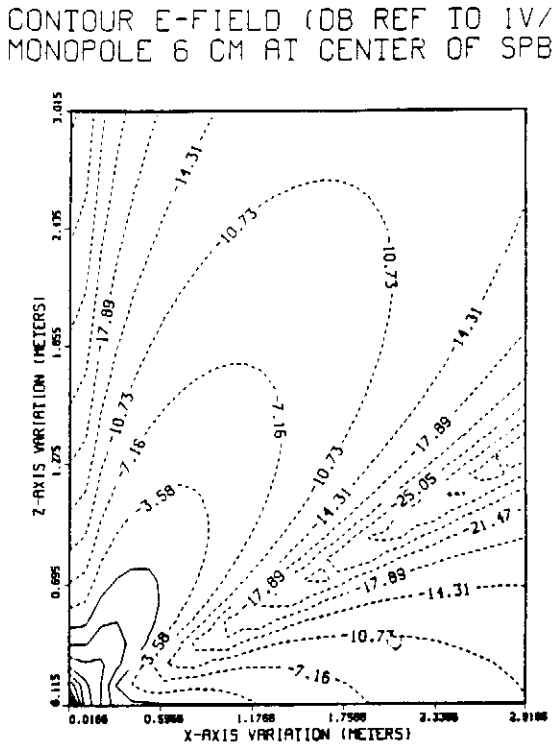

Figure 7a. Total E-Field Contours, Monopole at Patch Box Center.

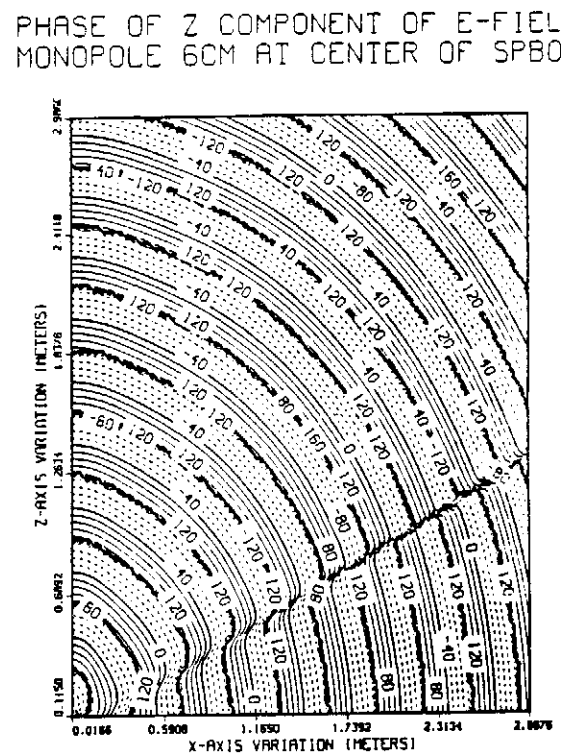

Figure 7b. Z-Component, E-Field Phase Contours, Monopole at Patch Box Center.

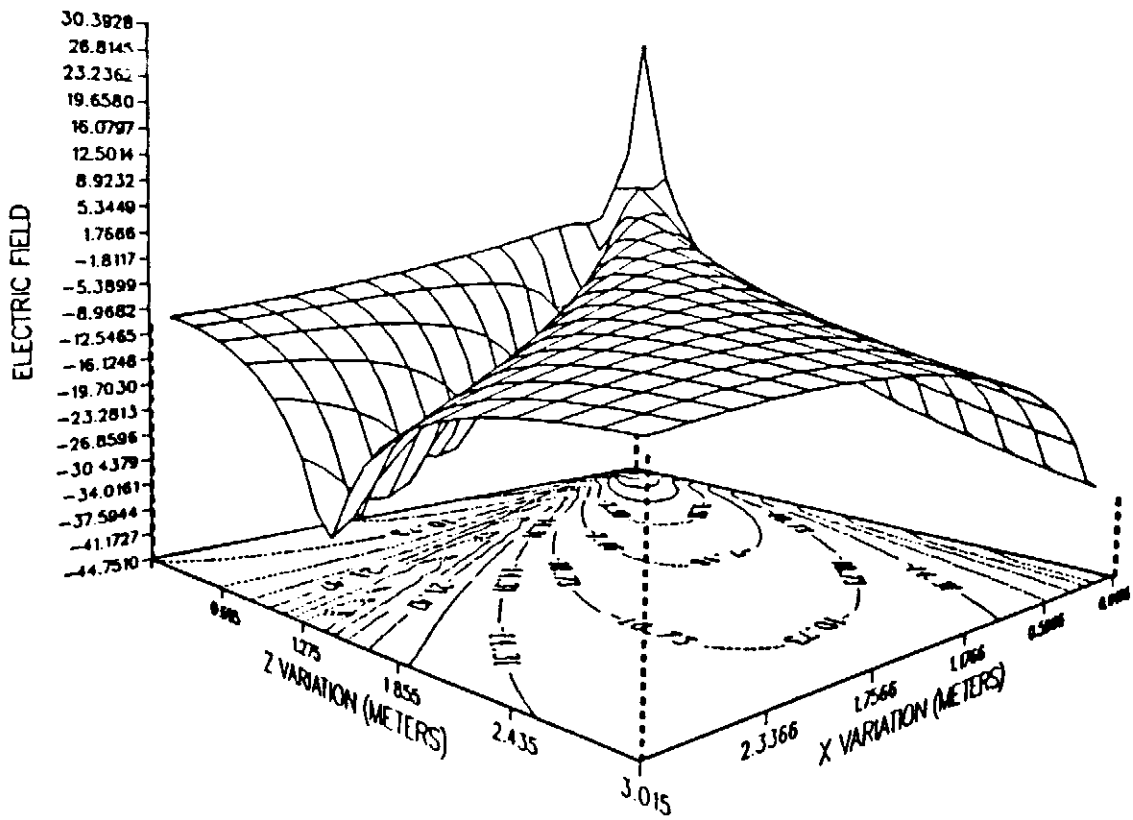

Figure 8. Total E-Field 3-D Plot, View Toward Monopole. Monopole at Patch Box Center.

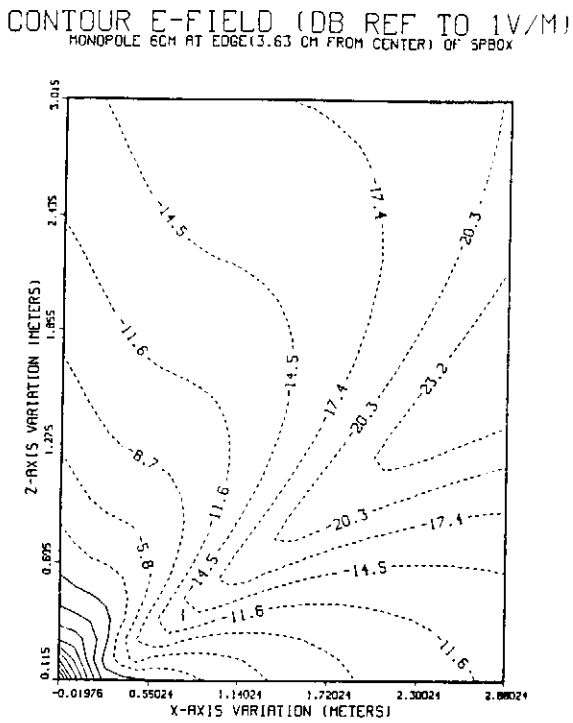

Figure 9a. Total E-Field Contours, Monopole at Patch Box Edge.

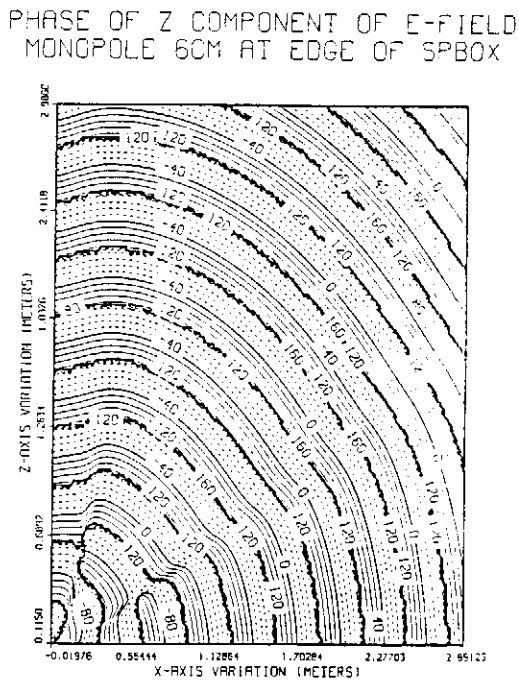

Figure 9b. Z-Component, E-Field Phase Contours, Monopole at Patch Box Edge.

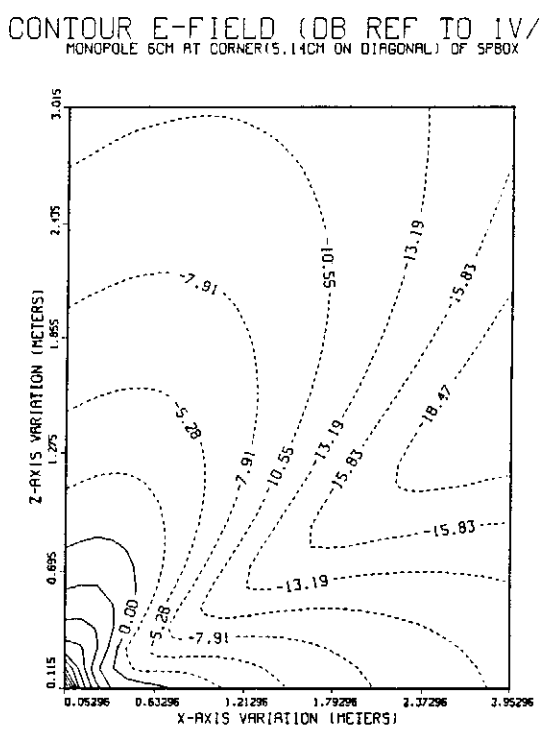

Figure 9c. Total E-Field Contours, Monopole at Patch Box Corner.

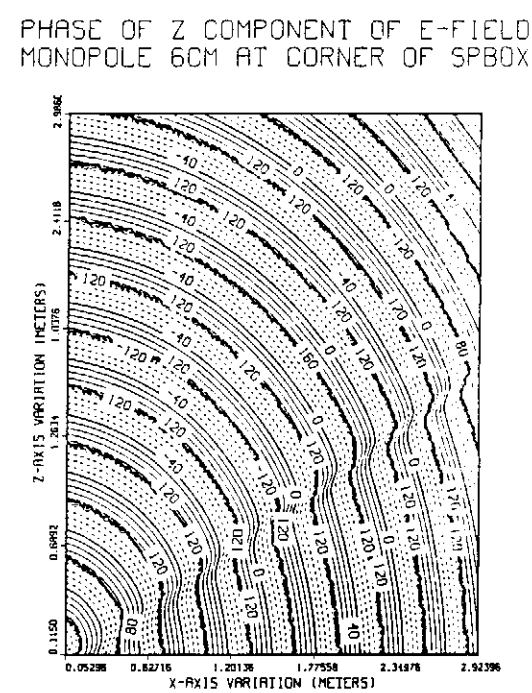

Figure 9d. Z-Component, E-Field Phase Contours, Monopole at Patch Box Corner.

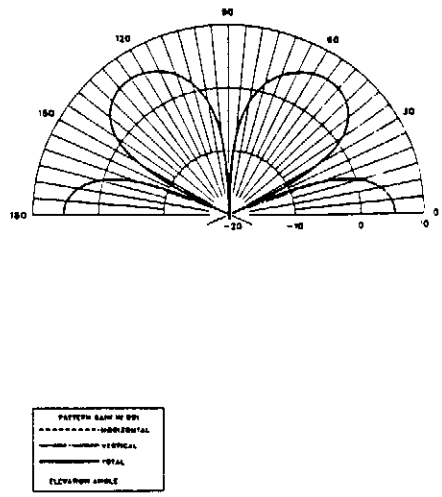

Figure 10a. Vertical Pattern, Monopole at Patch Box Center.

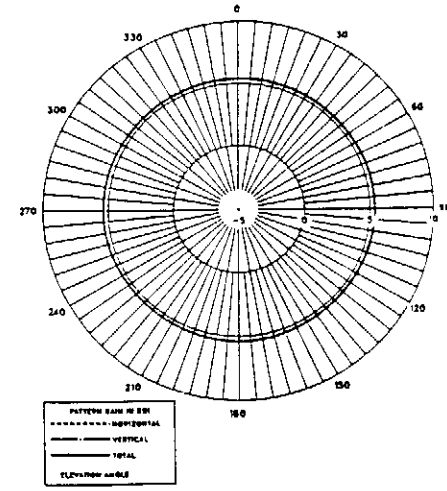

Figure 10b. Horizontal Pattern, Monopole at Patch Box Center.

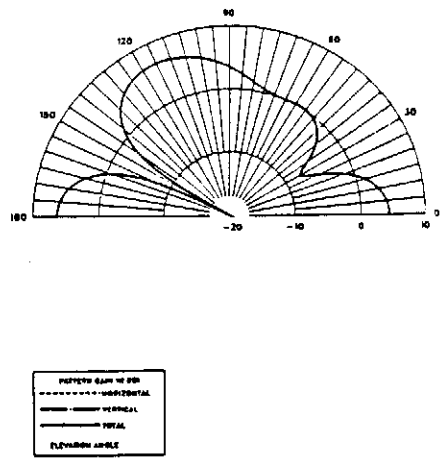

Figure 10c. Vertical Pattern, (X-Axis Cut), Monopole at Patch Box Edge.

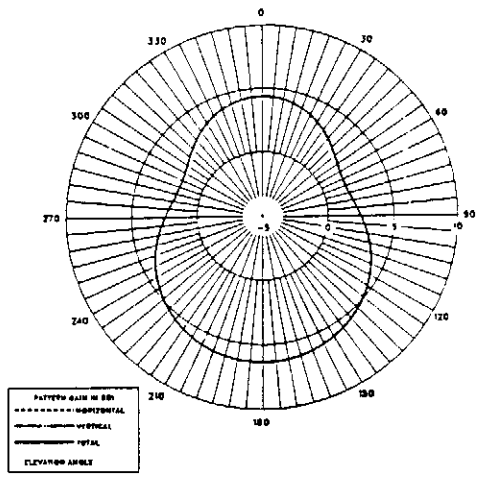

Figure 10d. Horizontal Pattern, Monopole at Patch Box Edge.

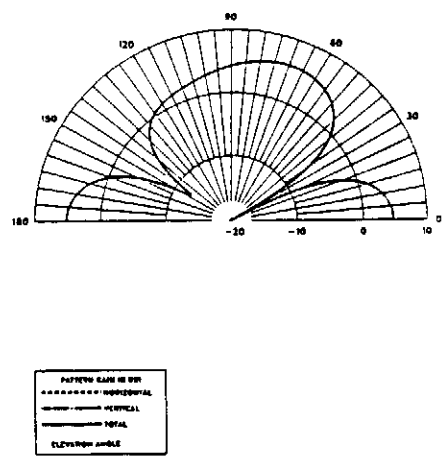

Figure 10e. Vertical pattern (45° Cut), Monopole at Patch Box Corner.

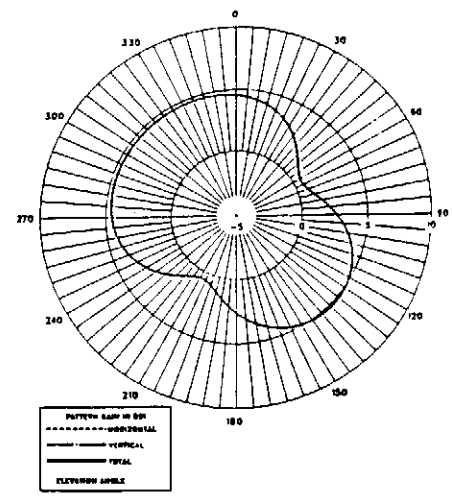

Figure 10f. Horizontal Pattern, Monopole at Patch Box Corner.

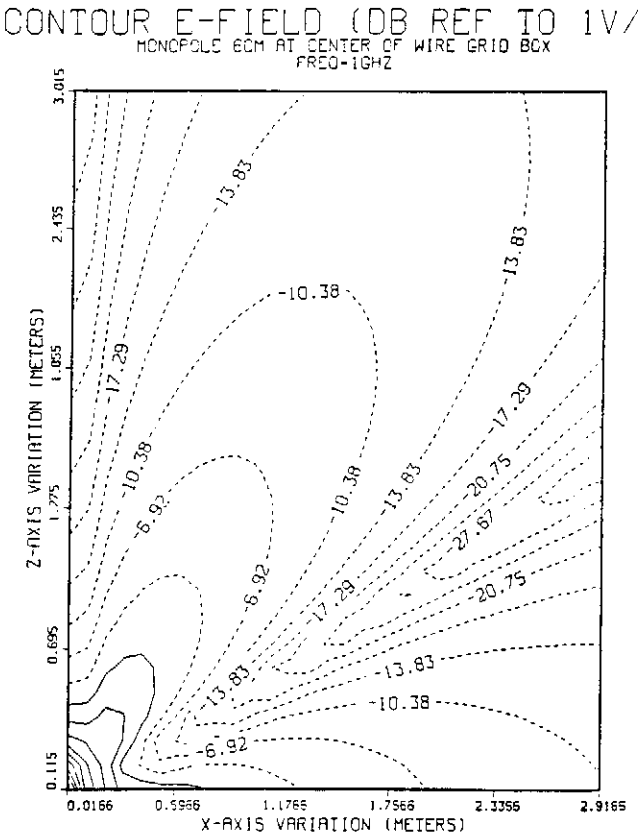

Figure 11a. Total E-Field Contours, Monopoles at Wire Grid Box Center.

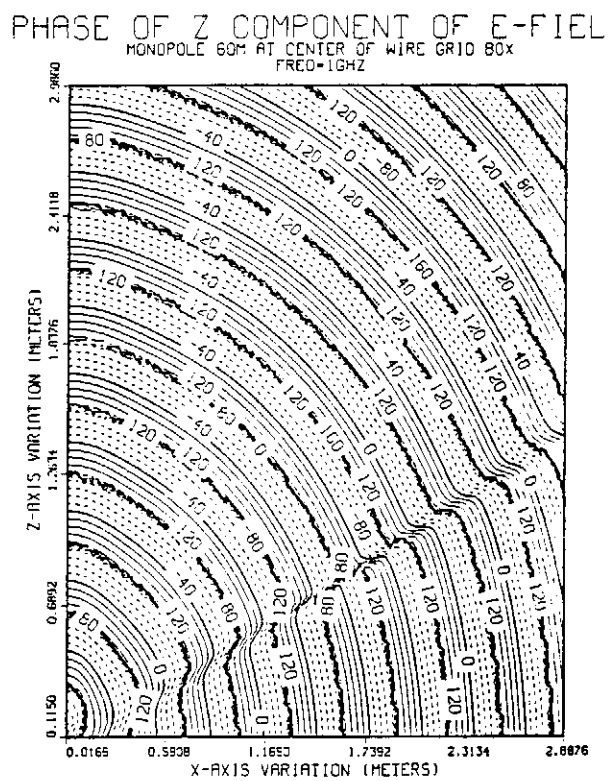

Figure 11b. Z-Component, E-Field Phase Contours, Monopole at Wire Grid Box Center.